Cavitation in ^{3}He-^{4}He liquid mixtures at low temperatures

Montserrat Guilleumas, Dora M. Jezek,* Martí Pi, and Manuel Barranco
Departament d'Estructura i Constituents de la Matèria, Facultat de Física, Universitat de Barcelona, E-08028 Barcelona, Spain

Jesús Navarro
Instituto de Física Corpuscular (Centre Mixt Consejo Superior de Investigaciones Científicas Universitat de València), Facultat de Física, E-46100 Burjassot, Spain

(Received 21 June 1994)

Bubble formation in solutions of ^{3}He and ^{4}He is studied within a density-functional approach. In particular, the temperature dependence of the cavitation pressure for different ^{3}He concentrations is calculated at low temperatures and compared to that of pure ^{4}He. The presence of Andreev states lowers the surface tension and, consequently, nucleation barriers are drastically reduced. This fact means that even at low ^{3}He concentrations the cavitation process takes place at higher pressures than the spinodal pressure, which is not the case for pure ^{4}He.

I. INTRODUCTION

This work is motivated by recent experiments[1–4] on cavitation in liquid ^{4}He, which have renewed the interest of theoreticians in the study of liquid helium properties at low temperature and negative pressure. These theoretical studies have been based on a density-functional approach,[2,3,5–7] which has proven to be very useful since it avoids important shortcomings inherent to the classical nucleation theory (see, for instance, Refs. 2, 7, 8). In particular, a density-functional approach correctly takes into account (i) the change in energy of a cluster due to curvature corrections, and (ii) the modification in the surface energy of a cluster due to the presence of vapor as temperature increases. Both changes are important for small size clusters.

One of the original reasons for employing helium to analyze cavitation is its immiscibility at low temperature. Indeed, at temperatures near absolute zero helium can be prepared free of impurities, and may thus provide a good test for homogeneous nucleation theories. In previous works[6,7,9] we have used a density-functional approach to investigate thermal nucleation and cavitation in each pure isotope. However, liquid helium is usually a mixture of ^{3}He and ^{4}He, and the aim of the present work is to complete these studies considering the case of mixtures.

A density functional for homogeneous mixtures at zero temperature has been constructed by Dalfovo and Stringari[10,11] and tested to describe some experimental data. We have employed the same functional, slightly modifying the surface parameters to better fit the experimental surface tension of pure ^{4}He and that of the mixture at saturation.

It is well known that at low temperature, even when small amounts of ^{3}He are present in ^{4}He, the surface tension of the liquid is considerably reduced.

This is due to the presence of ^{3}He atomic levels at the free surface of liquid ^{4}He, which are referred to as Andreev states.[12] We will show that the cavitation barrier strongly depends on surface tension, and bubble formation is enhanced even at very low ^{3}He concentrations. Therefore, a sizable change in the cavitation pressure with respect to that of the pure system should be observed. A lower bound to the minimum pressure a solution of ^{3}He in ^{4}He can attain as a metastable system is estimated. At this pressure, the probability of forming a critical bubble is high and the system is likely to split into two phases.

The present work is structured as follows. In Sec. II we analyze the homogeneous system to determine the boundaries between the metastable (where cavitation takes place) and the stable and unstable regions. In Sec. III we consider the inhomogeneous system, fixing the functional parameters to correctly fit the experimental surface tension of the ^{4}He liquid free surface and of the mixture at saturation. We also calculate the surface tension of the free surface of the mixture, which is relevant for bubble formation. In Sec. IV we consider cavitation. Using the density functional, calculations of the barrier height are performed as a function of pressure and ^{3}He concentration, which enable us to obtain the homogeneous cavitation pressure via thermal activation. Finally, in Sec. V we draw some conclusions.

II. METASTABILITY REGION

The following free energy density for a mixture of ^{3}He and ^{4}He has been used:[11]

$$f = f_v + \frac{\hbar^2}{2m_4}\tau_4 + \frac{\hbar^2}{2m_3^*}\tau_{3s} + d_4(\nabla\rho_4)^2 + d_3(\nabla\rho_3)^2 + d_{34}(\nabla\rho_3\cdot\nabla\rho_4), \quad (1)$$

with

$$f_v = \frac{1}{2}b_4\rho_4^2 + \frac{1}{2}c_4\rho_4^2\rho^{\gamma_4} + \frac{\hbar^2}{2m_3^*}\tau_{3v} + \frac{1}{2}b_3\rho_3^2 + \frac{1}{2}c_3'\rho_3^2\rho^{\gamma_3} + \frac{1}{2}c_3''\rho_3^{2+\gamma_3} + b_{34}\rho_3\rho_4 + c_{34}\rho_3\rho_4\rho^{\gamma_{34}}, \quad (2)$$

where ρ_i is the particle density of the ^{i}He isotope, ρ is the total density $\rho = \rho_3 + \rho_4$, and τ_i and m_i are the corresponding kinetic energy densities and atomic masses, respectively. The ^{3}He effective mass is defined as

$$m_3^* = m_3\left(1 - \frac{\rho_3}{\rho_{3c}} - \frac{\rho_4}{\rho_{4c}}\right)^{-2}, \quad (3)$$

and the kinetic energy densities are

$$\tau_4 = \frac{1}{4}\frac{(\nabla\rho_4)^2}{\rho_4} \quad (4)$$

and

$$\tau_3 = \tau_{3v} + \tau_{3s}, \quad (5)$$

where

$$\tau_{3v} = \frac{3}{5}(3\pi^2)^{2/3}\rho_3^{5/3}, \qquad \tau_{3s} = \frac{1}{18}\frac{(\nabla\rho_3)^2}{\rho_3} + \frac{1}{3}\Delta\rho_3. \quad (6)$$

We have considered that ^{3}He is in the normal phase and consequently, by "zero temperature" we shall always mean a temperature around 3 mK. Let us first consider a homogeneous mixture, in which the density gradient terms vanish and f reduces to f_v. The parameters $b_4, c_4, \gamma_4, b_3, \gamma_3, \rho_{3c}$ and the sum $c_3' + c_3''$ have been adjusted so as to reproduce various physical quantities at saturation for pure ^{4}He and ^{3}He homogeneous systems, such as the energy per particle, the density, the compressibility, and the ^{3}He effective mass. The parameters b_{34}, c_{34}, and c_3'' have been fixed in order to reproduce the maximum solubility of ^{3}He in ^{4}He at zero pressure, the ^{3}He chemical potential when $\rho_3 \to 0$, and the ratio of specific heats between ^{3}He and ^{4}He at the same limit. The parameter ρ_{4c} has been fixed to take into account the variation of m_3^* with ^{3}He concentration, and γ_{34} has been taken as an average between γ_3 and γ_4.[11] The values of these parameters are given in Table I.

Before studying cavitation, it is convenient to delimit the metastable region where nucleation occurs. At zero temperature (T), we determine its boundaries with the stable and unstable regions in the plane (P, x), where P is the pressure and x is the ^{3}He concentration ($x = \rho_3/\rho$). Necessary and sufficient stability conditions for a binary system[13,14] are given by the inequalities on the compressibility,

$$K = \left(\frac{\partial P}{\partial \rho}\right)_x \geq 0, \quad (7)$$

and the chemical potentials

$$\left(\frac{\partial \mu_4}{\partial x}\right)_P \leq 0 \text{ or } \left(\frac{\partial \mu_3}{\partial x}\right)_P \geq 0. \quad (8)$$

A positive compressibility guarantees mechanical stability, whereas the condition on the chemical potentials ensures diffusive stability. Taken as equalities, the above equations determine two curves on the (P, x) plane, which are shown in Fig. 1 as a dot-dashed and a dashed line, respectively. One can see in this figure that, for the functional we are using, the diffusive stability condition is always violated first, and so inequality (7) is in practice useless for this problem. Therefore, the spinodal line, which is the boundary between the metastable and the unstable regions, is fixed by the diffusive stability condition. This line will be denoted $P_{sp}(x)$. At $P = 0$, it cuts the x axis at $x_{sp} \sim 30\%$.

Comparison of x_{sp} with the maximum value of x, for which the mixture has been experimentally found in a metastable homogeneous state $x_h \simeq 15\%$,[15] can be considered as being rather dubious. This would mean that one is identifying the spinodal pressure with the homogeneous nucleation pressure, which is the only one that is experimentally accessible. As a matter of fact, these pressures can be quite different.[3,6,7] In the present case the functional has been fixed to reproduce x_0,[11] yielding an x_{sp} value above the experimental x_h at $P = 0$. The variational calculations of Ref. 16 yield $x_{sp} = 18\%$, and $x_0 = 1\%$ instead of the experimental value $x_0 \sim 6.5\%$.[15]

To draw the frontier between the metastable and the stable region let us first consider the maximum concentration curve which is determined by the two-phase equilibrium equations

$$P(\rho, x) = P(\rho_{3p}, x = 1) \quad (9)$$

and

TABLE I. Parameters of the density functional employed in this work.

b_4 (K Å^3)	c_4 (K Å$^{3+\gamma_4}$)	γ_4	b_3 (K Å^3)	$c_3' + c_3''$ (K Å$^{3+\gamma_3}$)	c_3'' (K Å$^{3+\gamma_3}$)	γ_3	ρ_{3c} (Å^{-3})
-888.81	1.04554×10^7	2.8	-683.0	1.405057×10^6	-5.0683×10^4	2.1	0.0406
ρ_{4c} (Å^{-3})	b_{34} (K Å^3)	c_{34} (K Å$^{3+\gamma_{34}}$)	γ_{34}	d_3 (K Å^5)	d_4 (K Å^5)	d_{34} (K Å^5)	
0.062	-777.29	4.564748×10^6	2.5	2222.0	2048.0	4400.0	

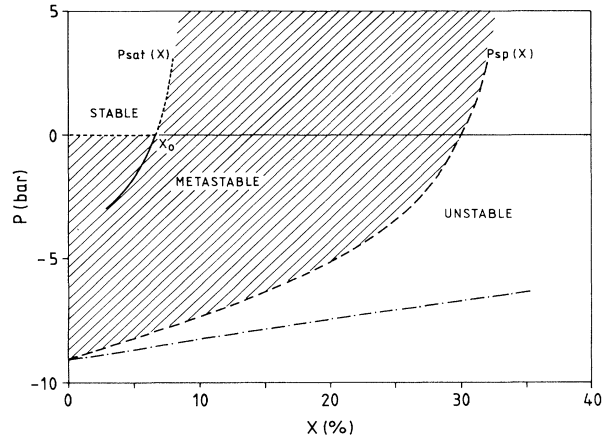

FIG. 1. Phase diagram of the mixture at $T = 0$.

$$\mu_3(\rho, x) = \mu_3(\rho_{3p}, x = 1), \tag{10}$$

where ρ_{3p} is the density of segregated ^{3}He. These equations determine a curve on the (P, x) plane which is denoted as $P_{\rm sat}(x)$ in Fig. 1. It is interesting to note that Eqs. (9) and (10) have solutions at negative pressures.

At a given positive pressure P, for concentrations larger than those defined by the equation $P = P_{\rm sat}(x)$, the single-phase system is metastable because the two-phase system (pure ^{3}He and a saturated mixture) has a lower free energy, where the formation of critical ^{3}He drops is important as they are responsible for phase separation.

Another metastability, which is the one we are interested in, arises from the application of a negative pressure (tensile strength). In this case, the system will develop either a free surface for low concentrations, or ^{3}He will segregate and also produce a mixture-pure ^{3}He interface. In the first case, phase separation will proceed by bubble nucleation, and in the second case by ^{3}He drop nucleation. $P_{\rm sat}(x)$ is interrupted at the ^{3}He spinodal pressure,[5] as for lower pressures the above equations are meaningless.

Finally, the boundary between the metastable and the stable regions is determined by the line $P = 0$ from $x = 0$ up to $x_{\rm sat}$ (which we shall call x_0), and the curve $P_{\rm sat}(x)$ for $x > x_0$. We have indicated it by the the short-dashed line in Fig. 1. The metastable zone is the hatched region in this figure.

III. INHOMOGENEOUS SYSTEM: SURFACE TENSION

To analyze the properties of the inhomogeneous system, the full free energy density in Eq. (1) has to be considered. The parameters d_3, d_4, and d_{34} have been determined by fitting the experimental surface tensions, and they are given in Table I. Our values differ slightly from those of Ref. 11, since we have tried to reproduce the experimental data of Refs. 17, 18 instead of those of Ref. 19 used by Dalfovo.[11]

Liquid helium mixtures at equilibrium may develop two kind of interfaces. One corresponds to the liquid free surface, and it appears at $P = 0$ when $x < x_0$. The other one appears when ^{3}He segregates for $x \geq x_0$ and $P \geq 0$, forming a pure ^{3}He-mixture interface. Different surface tensions are associated with both of these interfaces.

For $x < x_0$ at $P = 0$, the density profiles $\rho_3(z)$ and $\rho_4(z)$ are obtained by solving the coupled Euler-Lagrange (EL) equations

$$\frac{\delta f}{\delta \rho_3} = \frac{\partial f}{\partial \rho_3} - \nabla \frac{\partial f}{\partial(\nabla \rho_3)} = \mu_3 \tag{11}$$

and

$$\frac{\delta f}{\delta \rho_4} = \frac{\partial f}{\partial \rho_4} - \nabla \frac{\partial f}{\partial(\nabla \rho_4)} = \mu_4, \tag{12}$$

with the condition that the densities tend to zero when $z \to -\infty$. When $z \to +\infty$ the densities tend to values of ρ_3 and ρ_4 such that $P(\rho_3, \rho_4) = 0$ and $x = \rho_3/(\rho_3 + \rho_4)$.

The surface tension is calculated as

$$\sigma = \int_{-\infty}^{\infty} \Big[f(z) - \mu_3 \rho_3(z) - \mu_4 \rho_4(z) + P_{\rm eq} \Big] dz$$
$$\equiv \int_{-\infty}^{\infty} \Big(P_{\rm eq} - p(z) \Big) dz \,, \tag{13}$$

where $P_{\rm eq}$ is the equilibrium pressure, $P_{\rm eq} = p(z \to \pm\infty)$. Dalfovo[11] has calculated the surface tension between pure ^{3}He and the saturated mixture using a family of Wood-Saxon densities by fixing the parameter d_{34} to the value of $d_3 + d_4$. In particular, for $P_{\rm eq} = 0$ a value of $\sigma = 0.026$ K Å^{-2} was obtained, while extrapolation of the experimental values yields around 0.016 K Å^{-2}.[19]

The EL equations have been solved for $x = x_0$. The boundary conditions for $z \to \pm\infty$ are obtained by solving the two-phase equilibrium conditions (9) and (10). The value of the parameter d_{34} has been varied so as to reproduce as well as possible the experimental surface tension of the mixture-pure ^{3}He interface at $P_{\rm eq} = 0$. The best result obtained for σ is 0.018 K Å^{-2}, and the full set of parameters defining the functional is given in Table I.

We have also calculated the surface tension $\sigma(x)$ pertaining to the free surface of the mixture, which is the one relevant in classical cavitation theories. In Fig. 2 we show it as a function of concentration. One can see that σ decreases abruptly near $x = 0$ (for pure ^{4}He, the surface tension is 0.256 K Å^{-2}). It is related to the presence of a finite surface density (N_s) of ^{3}He atoms at the interface. It is shown in Fig. 3(a), where the density profile for $x = 0.05\%$ is plotted. This fact was predicted by Andreev[12] as a sign of the existence of ^{3}He surface states with larger binding energy than those of a ^{3}He atom in the ^{4}He liquid bulk.

In a recent work, Pavloff and Treiner[20] have studied, using the original functional of Ref. 11, the properties of the two-dimensional system formed by ^{3}He atoms on the surface of liquid ^{4}He as a function of the ^{3}He coverage

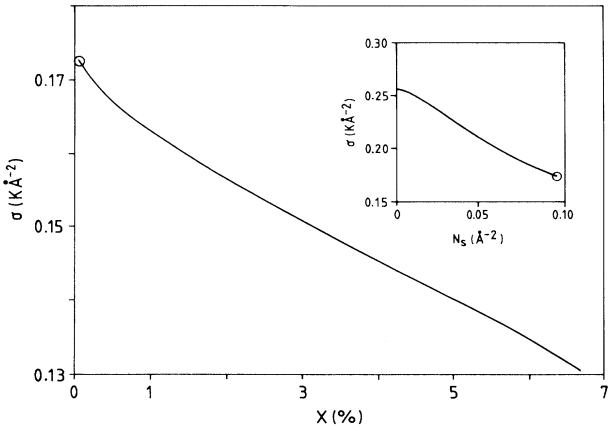

FIG. 2. Surface tension σ plotted as a function of the ^{3}He concentration x. In the upper right-hand corner we show σ as a function of the ^{3}He surface density N_s. The configuration corresponding to the final value of N_s (0.095 Å^{-2}) and to the first value of x (0.05%) are approximately equivalent, both yielding $\sigma = 0.172$ K Å^{-2}.

N_s. They find several types of surface states accessible to ^{3}He atoms and calculate the variation of the surface tension as a function of N_s. We have repeated this calculation and found similar results (remember we are using a different parameter set), which are shown in the upper right-hand corner of Fig. 2. The last N_s of this graph (N_s=0.095 Å^{-2}) roughly corresponds to the first calculation in x ($x = 0.05\%$) in the sense that both yield very similar ^{3}He density profiles at the surface.

For increasing values of x, the maximum of ρ_3 at the surface smoothly increases until it reaches its equilibrium value (see Fig. 3). As one would expect, when x approaches the calculated saturation value $x_0 = 6.6\%$ at $P = 0$, the so-called Antonov rule[18] holds, i.e.,

$$\sigma = \sigma_3 + \sigma_i \,, \tag{14}$$

where σ, σ_3, and σ_i, are the surface tensions of the free liquid mixture at saturation, of pure liquid ^{3}He, and of the interface between pure liquid ^{3}He and the saturated mixture, respectively. The numerical values of these quantities for $x = 6.6\%$ are 0.131, 0.113, and 0.018 K Å^{-2}, thus perfectly fulfilling the above relation. The corresponding density profile is shown in Fig. 3(c).

For $x \geq x_0$, in accordance with experiment,[21] no solution to Eqs. (11),(12) exists: It is impossible to observe a supersaturated mixture with a liquid free surface, since the exceeding ^{3}He segregates to the surface.

IV. CAVITATION

A metastable system may be stable with respect to small variations of the internal parameters, in particular with respect to the formation of small new phase nuclei. The stable state is separated from it by a nucleation barrier, which may be overcome either by thermal fluctuations or by quantum tunneling for low enough temperatures.[22] The barrier height is determined by the free energy of the critical nucleus, which is such that with any further infinitesimal increase in size, it can continue to grow without any external intervention and trigger the phase separation. This happens, for instance, in a supersaturated vapor in which liquid droplets nucleate. The case we are interested in is that of a liquid (with $x < x_0$) submitted to a tensile strength in which bubbles are formed.

The so-called capillarity model can provide a rough idea about the role played by the surface tension in the nucleation process. Sharp surface nuclei of radius R are assumed and the free energy is written as

$$U(R) = 4\pi\sigma R^2 + \frac{4}{3}\pi R^3 \Delta P \,, \tag{15}$$

where ΔP is the difference in pressure between the nucleus and the bulk.

The barrier height is determined by the maximum value of $U(R)$, which occurs at a size $R_{\max} = 2\sigma/|\Delta P|$, and is equal to

$$U_{\max} = \frac{16\pi\sigma^3}{3(\Delta P)^2} \,. \tag{16}$$

In the case of bubbles we assume the density inside is zero, so that $\Delta P = P$.

The nucleation rate, i.e., the number of bubbles formed in the homogeneous system per unit of time and of volume due to thermal fluctuations, is given by

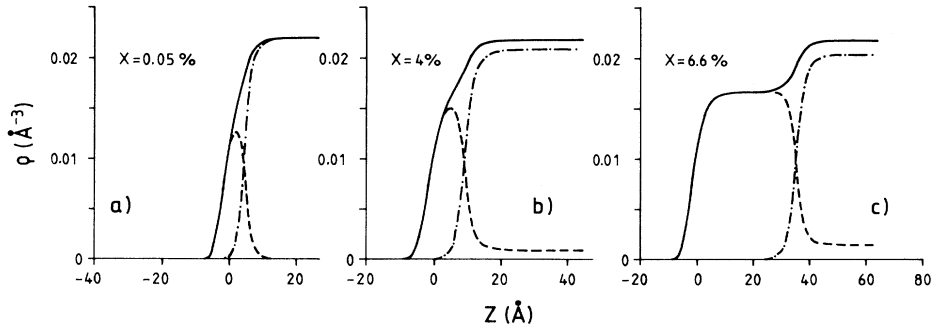

FIG. 3. Liquid free surface density profiles as a function of z for different ^{3}He concentrations: (a) $x = 0.05\%$, (b) $x = 4\%$, and (c) $x = 6.6\%$. Dashed lines correspond to ^{3}He, dot-dashed lines to ^{4}He, and solid lines to the total density of the mixture ($z = 0$ is defined as the point where $\rho = \rho_{\rm sat}/2$).

$$J_T = J_{0T} \exp^{-U_{\max}/kT}, \tag{17}$$

where k is Boltzmann's constant and the preexponential factor J_{0T} depends on the dynamics of the cavitation process. To make a quantitative estimate of the cavitation pressure P_h, one may proceed as in Refs. 2, 7, that is, consider a rate $J_T = 1\ \mathrm{cm}^{-3}\,\mathrm{s}^{-1}$ and solve the equation

$$\frac{U_{\max}}{kT} = \ln J_{0T}\ (\mathrm{cm}^{-3}\,\mathrm{s}^{-1}). \tag{18}$$

Although expression (16) for the barrier is valid only near saturation, it gives an idea on the dependence of the nucleation rate upon surface tension. This strong dependence suggests that nucleation is enhanced when ^{3}He is solved in ^{4}He due to the decrease of σ.

To obtain an estimate of the relative departure between spinodal and nucleation pressures at $x = 0$ and at any other x value, we can use the barrier height approximation near the spinodal given by Lifshitz and Kagan[22] whose dependence on P and σ through x is

$$U_{\max} \sim \sigma^3(x)\ [P(x) - P_{\mathrm{sp}}(x)]^{3/4}. \tag{19}$$

Solving (18) for both concentrations at the same temperature and taking the quotient we obtain

$$\frac{P_h(x) - P_{\mathrm{sp}}(x)}{P_h(0) - P_{\mathrm{sp}}(0)} \simeq \left(\frac{\sigma(0)}{\sigma(x)}\right)^4. \tag{20}$$

Since $\sigma(x)$ changes sizeably even at very low concentration, the cavitation pressure will differ appreciably from that of pure ^{4}He. For example, this ratio is 4.5 for $x = 10^{-4}\%$ and 6 for $x = 1\%$. This means that at the same temperature, the cavitation pressure for $x = 10^{-4}\%$ (1%) is 4.5 (6) times farther away from the spinodal pressure than for pure ^{4}He.

As has been already discussed by Xiong and Maris,[2] the approximations for calculating the barrier height near saturation (16) and near the spinodal (19) cannot be interpolated in a natural way, and a more accurate treatment is needed to describe cavitation throughout the pressure range. The approach used is based on a formalism proposed earlier by Cahn and Hilliard,[23,24] and later developed by various authors,[2,7,25] whose basic tool is a density functional. One has to solve the EL equations (11) and (12) in spherical coordinates, where the bubble density profiles depend only on r, and $\mu_{3(4)}$ are the corresponding chemical potentials in the homogeneous metastable system. The boundary conditions are that the r derivative of $\rho_{3(4)}$ at $r = 0$ is zero and that $\rho_{3(4)}(r \to \infty)$ approaches the corresponding densities of the metastable system $\rho_{3m(4m)}$. The nucleation barrier height $\Delta\Omega$ is then obtained from the difference between the grand potential of the critical cluster and that of the homogeneous metastable state:

$$\Delta\Omega = \int d\mathbf{r}\Big(f(\rho_3,\rho_4) - f(\rho_{3m},\rho_{4m}) - \mu_3(\rho_3 - \rho_{3m}) - \mu_4(\rho_4 - \rho_{4m})\Big). \tag{21}$$

Remember that since the metastable system is homogeneous,

$$P = -f_v(\rho_{3m},\rho_{4m}) + \mu_3\rho_{3m} + \mu_4\rho_{4m}. \tag{22}$$

In Fig. 4 we have plotted these barriers as a function of P for several ^{3}He concentrations. Their P dependence is as expected:[2,6,7] $\Delta\Omega$ diverges when P goes to zero (not shown in Fig. 4), and drops to zero at the corresponding spinodal pressure. It is worth mentioning two new aspects appearing in the case of He mixtures which are absent in the case of pure liquid He. First, in the metastable $P < 0$ region not only bubbles, but also ^{3}He droplets may be formed. Actually, for $x \lesssim x_0$ and $P \lesssim 0$ we have already found both kind of configurations. As is expected, the barriers for nucleating bubbles are smaller, but at higher concentrations they are higher. Second, the P dependence of $\Delta\Omega$ for ^{3}He drops being formed in the mixture is different to that for bubbles. In the case of drops, at a given x the barrier $\Delta\Omega$ diverges at the negative P obtained when one solves the equilibrium conditions (9) and (10). These facts are originated by the limited solubility of ^{3}He in ^{4}He liquid at $T \sim 0$ K.

Figure 4 clearly shows the effect on $\Delta\Omega$ of increasing the ^{3}He concentration, and thus on the nucleation rate. Even concentrations as small as $10^{-4}\%$ cause a sizable effect (recall commercial helium contains about 1.4×10^{-4} % of ^{3}He).

To obtain the thermal nucleation rate one has to use $\Delta\Omega$ instead of $U_{\max}$ in Eq. (17). Strictly speaking, one should calculate $\Delta\Omega$ as a function of T. However, for the low temperatures we are considering, no appreciable modifications in the density functional are expected to arise. It is important to recall that the solubility of ^{3}He in ^{4}He drastically increases with T, and has important consequences on $\sigma(x)$. From the analysis of the available experimental data,[26] we estimate that the present calculations are reliable up to $T \simeq 150$ mK. To obtain the

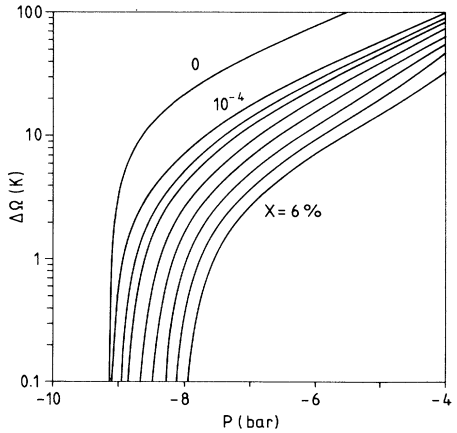

FIG. 4. From top to bottom, cavitation barriers as a function of P for pure ^{4}He and for ^{3}He concentrations $x = 10^{-4}\%$, 0.5%, and 1%–6%.

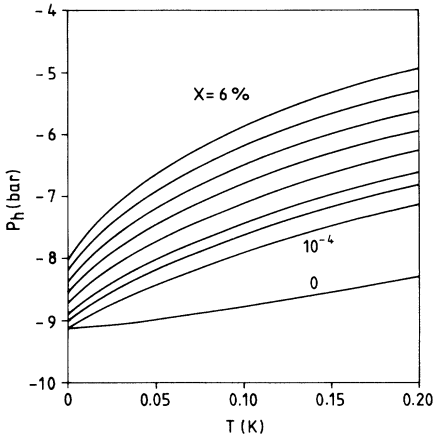

FIG. 5. Homogeneous cavitation pressure P_h as a function of temperature for the same ^{3}He concentrations as in Fig. 4 (from bottom to top).

homogeneous cavitation pressure P_h via thermal fluctuations we have solved Eq. (18), with the improved barrier height $\Delta\Omega$, taking the same value as in Ref. 7 for J_{0T}.

In Fig. 5, P_h is displayed as a function of T and x. For $T = 0$ the cavitation pressure corresponds to the spinodal one (we have neglected quantum fluctuations). One can see that for the lower concentration ($x = 10^{-4}$ %), the differences with pure ^{4}He are appreciable, ranging from ~ 0.5 bar at $T = 0.05$ K to ~ 1 bar at $T = 0.2$ K.

Comparing the spinodal and cavitation pressures qualitative agreement with (20) is seen. For example, at $T = 100$ mK, the difference between spinodal and cavitation pressure is 0.3 bar for pure ^{4}He, and 1.3 bar for $x = 1\%$.

By simple inspection of Fig. 5 we may infer that for temperatures above the $T \simeq 0$ region where cavitation is produced via quantum tunneling, the process occurs away from the spinodal pressure, so that none of the two approximations proposed by Lifshitz and Kagan[22] (i.e., near the spinodal or near saturation) apply here.

Finally, in Fig. 6 we display a sequence of bubble profiles for $x = 4\%$ and pressures $P = -7$, -5, -4, and -2 bar. Near the saturation pressure, bubbles are large in size and empty, with a ^{3}He shell located at the surface. When the pressure becomes more negative, the size of critical bubbles diminishes, and bubbles are first filled with ^{3}He before ^{4}He starts flowing in. The complicated morphology of these curves suggests that any schematic assumption about the shape of the density profiles in the study of cavitation is extremely complicated, whereas the density-functional approach constitutes a reliable and affordable way of tackling this problem.

V. CONCLUSIONS

In this paper we have extended our previous work on thermal cavitation in liquid ^{3}He and ^{4}He to the case of mixtures. This has led to a rather detailed study of their surface properties. Due to the lowering of the surface tension with increasing ^{3}He concentration, cavitation is more likely to occur, and even for a concentration as small as 10^{-4}%, which is close to that of commercial helium, the pressure of thermal homogeneous cavitation is increased by about 1 bar with respect to that of pure ^{4}He. We have also found that the homogeneous cavitation pressure differs from the spinodal pressure a lot more in the mixture than in the pure system.

These effects are due to the presence of ^{3}He surface states, which also favor the formation of vortices in the

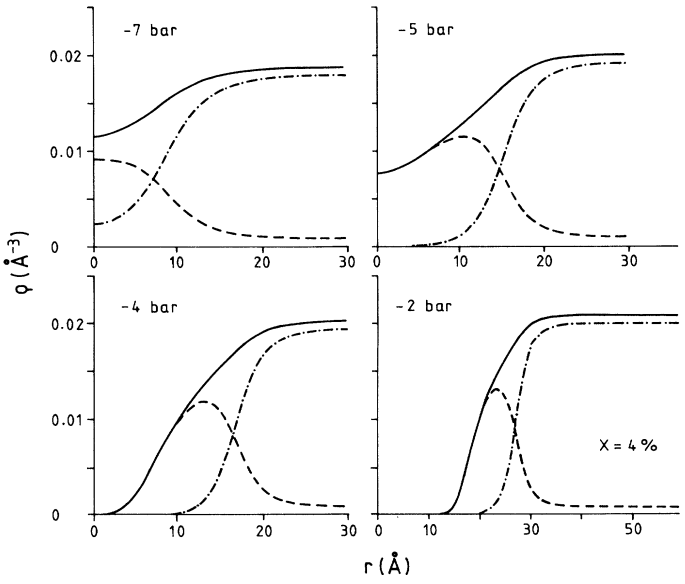

FIG. 6. Density profiles corresponding to the critical bubbles for $P = -7$, -5, -4, and -2 bar. The ^{3}He concentration is $x = 4\%$.

mixture, as may be seen by analyzing the influence of surface tension on the energetics of a vortex using the simple hollow core model.[27]

Below a crossover temperature T^*, which has not been reliably estimated so far, nucleation will proceed via quantum tunneling (QT), and for a given x the nucleation rate will be T independent. In their classic paper, Lifshitz and Kagan[22] derived two formulas to study QT based on the same approximations that have led to Eqs. (16) and (19). We have shown that unfortunately neither of them apply here.

Experimentally, the situation seems to be clearer for the case of ^{3}He drop formation in supersaturated mixtures, for which Satoh *et al.*[28] have determined that $T^* \simeq 10$ mK. An experimental determination of T^* for cavitation would render our calculations complete in the whole range of temperatures from 200 mK down to 3 mK, since below T^* the pressure of homogeneous cavitation is constant for a given x value. More precise measurements of the surface tension associated with the saturated liquid ^{3}He-mixture interface at $T \sim 0$ K would allow one to better estimate the value of the functional parameters.

Very recently, Burmistrov *et al.*[29] have developed a formalism for QT which takes into account dissipation and superfluidity, and have applied it to describe nucleation of ^{3}He drops in a supersaturated mixture to obtain the demixing curve. However, they make use of the capillarity approximation.

Possible extensions of the present study are to consider the presence of vortices in the mixture, and to study ^{3}He drop formation at $P \geq 0$ for $x \geq x_0$.[30] Work in these directions is now in progress.

ACKNOWLEDGMENTS

This work has been supported by DGICYT (Spain) Grant Nos. PB92-0761 and PB92-0820. D.M.J. thanks the CICYT (Spain), and M.G. the Departament d'Ensenyament of the Generalitat de Catalunya, for financial support. We thank the generous computer support of the CESCA facility.

* Permanent address: Departamento de Física, Facultad de Ciencias Exactas y Naturales, Universidad de Buenos Aires, RA-1428 Buenos Aires, Argentina.

[1] J.A. Nissen, E. Bodegom, L.C. Brodie, and J.S. Semura, Phys. Rev. B **40**, 6617 (1989).
[2] Q. Xiong and H.J. Maris, J. Low Temp. Phys. **77**, 347 (1989).
[3] Q. Xiong and H.J. Maris, J. Low Temp. Phys. **82**, 105 (1991).
[4] M.S. Pettersen, S. Balibar, and H.J. Maris, Phys. Rev. B **49**, 12 062 (1994).
[5] M.A. Solís and J. Navarro, Phys. Rev. B **45**, 13 080 (1992).
[6] M. Guilleumas, M. Pi, M. Barranco, J. Navarro, and M.A. Solís, Phys. Rev. B **47**, 9116 (1993).
[7] D.M. Jezek, M. Guilleumas, M. Pi, M. Barranco, and J. Navarro, Phys. Rev. B **48**, 16 582 (1993).
[8] D.W. Oxtoby, J. Phys. Condens. Matter **4**, 7627 (1992).
[9] J. Navarro, M. Guilleumas, M. Pi, M. Barranco, and M.A. Solís, in *Condensed Matter Theories*, edited by J.W. Clark and M. Sadiq (Nova Science, New York, 1994), Vol. 9.
[10] F. Dalfovo and S. Stringari, Phys. Lett. **112A**, 171 (1985).
[11] F. Dalfovo, Ph. D. thesis, University of Trento, 1989.
[12] A.F. Andreev, Zh. Eksp. Teor. Fiz. **50**, 1415 (1966) [Sov. Phys. JETP **23**, 939 (1966)].
[13] L. Landau and E. Lifshitz, *Física Estadística* (Ed. Reverté, Barcelona, 1969).
[14] K. Binder, in *Material Science and Technology*, edited by R.W. Cahn, P. Haasen, and E.J. Kramer (VCH, Germany, Weinheim, 1991), Vol. 5.
[15] C. Ebner and D.O. Edwards, Phys. Rep. **2**, 77 (1970).
[16] E. Krotscheck and M. Saarela, Phys. Rep. **232**, 1 (1993).
[17] M. Iino, M. Suzuki, and A.J. Ikushima, J. Low Temp. Phys. **61**, 155 (1985).
[18] H.M. Guo, D.O. Edwards, R.E. Sarwinski, and J.T. Tough, Phys. Rev. Lett. **27**, 1259 (1971).
[19] D.O. Edwards and W.F. Saam, in *Progress in Low Temperature Physics*, edited by D.F. Brewer (North-Holland, Amsterdam, 1978), Vol. VII A, p. 283.
[20] N. Pavloff and J. Treiner, J. Low Temp. Phys. **83**, 15 (1991).
[21] J. Landau, J.T. Tough, N.R. Brubaker, and D.O. Edwards, Phys. Rev. Lett. **23**, 283 (1969).
[22] I.M. Lifshitz and Yu. Kagan, Zh. Eksp. Teor. Fiz. **62**, 385 (1972) [Sov. Phys. JETP **35**, 206 (1972)].
[23] J.W. Cahn and J.E. Hilliard, J. Chem. Phys. **28**, 258 (1958).
[24] J.W. Cahn and J.E. Hilliard, J. Chem. Phys. **31**, 688 (1959).
[25] X.C. Zeng and D.W. Oxtoby, J. Chem. Phys. **95**, 5940 (1991).
[26] D.O. Edwards, S.Y. Shen, J.R. Eckardt, P.P. Fatouros, and F.M. Gasparini, Phys. Rev. B **12**, 892 (1975).
[27] F. Dalfovo, G. Renversez, and J. Treiner, L. Low Temp. Phys. **89**, 425 (1992).
[28] T. Satoh, M. Morishita, M. Ogata, and S. Katoh, Phys. Rev. Lett. **69**, 335 (1992).
[29] S.N. Burmistrov, L.B. Dubovskii, and V.L. Tsymbalenko, J. Low Temp. Phys. **90**, 363 (1993).
[30] J. Bodensohn, S. Klesy, and P. Leiderer, Europhys. Lett. **8**, 59 (1989).